Wide-Band Reduced-Size Uniplanar Magic-T, Hybrid-Ring, and de Ronde's CPW-Slot Couplers

Lu Fan, Chien-Hsun Ho, Sridhar Kanamaluru, *Student Member, IEEE*, and Kai Chang, *Fellow, IEEE*

Abstract— **New reduced-size uniplanar magic-T and hybrid-ring coupler suitable for MIC's and MMIC's have been developed using a CPW-slotline ring that is 20% smaller than comparable designs. These circuits provide good amplitude and phase characteristics over a broad bandwidth. Experimental results show that the hybrid-ring coupler has a 1.3 octave bandwidth centered at 4 GHz and the magic-T has a bandwidth of 1.6 octave from 2–6 GHz. Both have a maximum power dividing imbalance of 0.4 dB and a 2.5° maximum phase imbalance. Also a new uniplanar de Ronde's CPW-slot directional coupler was developed with good performance. The even-odd mode analysis of four-port networks with double symmetry was used to analyze this coupler. A de Ronde's coupler with 5 dB coupling was designed and demonstrated over the frequency range of 2.4–3.4 GHz. The measurement results agree with the theoretical design.**

I. Introduction

In the last few years, uniplanar transmission lines such as coplanar waveguide (CPW), slotline and coplanar strip (CPS) are becoming a competitive alternative to microstrip in many applications (including both microwave hybrid and monolithic technologies). These transmission lines are preferred because of their small dispersion, simple realization of short circuited ends, easy integration with lumped elements or active components, and circumventing the need for via holes. Many attractive components using uniplanar structures have been reported [1]–[5]. Some circuit configurations using uniplanar 180 and 90° hybrids were also proposed in [6]–[8]. This paper presents uniplanar hybrid coupler components that have characteristics similar to those of the microstrip circuits with the advantages of a uniplanar structure and better performance.

Hybrid couplers and magic-Ts are fundamental and important components used for microwave and monolithic integrated circuits. However, most of them are traditionally constructed with quarter-wavelength transmission lines, occupy large areas in MMIC's, and the bandwidths are limited due to the electrical line lengths. To miniaturize the hybrids and magic-Ts for monolithic integration, several attempts have already been made to reduce the size of the well known 1.5 λ_g circumference microstrip rat-race coupler [9], [10]. However, this reduction has led to narrowband operation.

To achieve small size and wide band operation, this paper presents a novel reduced-size uniplanar magic-T and a reverse-phase uniplanar hybrid-ring coupler, both using a CPW-slotline ring. These circuits are small in size (circumference is only $0.8\lambda_g$) and have broadband operation. In addition, a new uniplanar de Ronde's CPW-slotline directional coupler is also described with good amplitude characteristics and phase balance. The circuit analyses for the uniplanar hybrid couplers are based on simple transmission line circuit models used in Touchstone. The measured results agree with the theoretical predictions very well.

Manuscript received February 24, 1995; revised July 12, 1995. This work was supported in part by the U.S. Army Research Office, the NASA Center for Space Power, and the State of Texas Higher Education Coordinating Board's Advanced Technology Program.

The authors are with the Department of Electrical Engineering, Texas A&M University, College Station, TX 77843-3128 USA.

IEEE Log Number 9415485.

II. Reduced-Size Uniplanar Magic-T

Magic-T's are widely used as 0 and 180° power dividers or combiners in microwave circuits such as balanced mixers, amplifiers and frequency discriminators. Uniplanar magic-Ts are preferred for planar microwave integrated circuits because they allow easy series and shunt connections of passive and active solid-state devices without via holes [11]–[14]. However, the precision fabrication required for the three in-phase designs in [11] makes the circuit difficult to manufacture. In [14], the feed port is a slotline which is not convenient for most applications. The coupler design in [12], [13] is based on quarter wavelength sections that limit the bandwidth.

This section first describes the fundamental characteristics of the out-of-phase CPW-slotline T-junction which uses a CPW-slotline back-to-back transition to achieve a 180° phase reversal at the two output ports. A new uniplanar magic-T will then be presented with its equivalent circuit and design principles. Since the out-of-phase of the CPW- slotline T-junction is frequency independent (broad bandwidth), the resulting magic-T has a broad bandwidth with good performance.

A. CPW-Slotline Tee Junctions

The CPW-slotline T-junctions described here serves as a mode conversion between CPWs and slotlines. Fig. 1 shows the circuit configuration and schematic diagram of the E-field distribution for in-phase and out-of-phase T-junctions. The out-of-phase tee junction consists of one CPW tee junction and two CPW-slotline transitions. The arrows shown in Fig. 1 indicate the electric fields in the CPWs and slotlines. For the out-of- phase case shown in Fig. 1(b), the E-fields in the two arms of the CPW tee are directed towards the CPW center

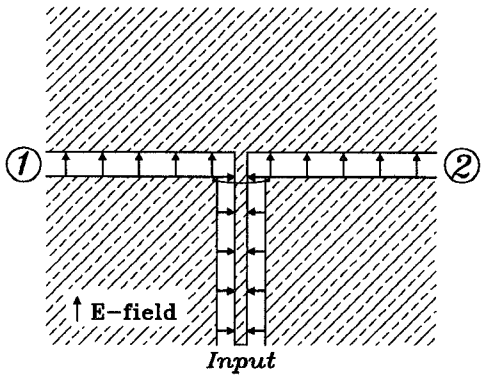

(a)

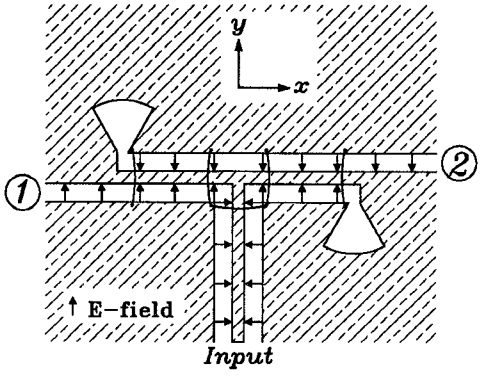

(b)

Fig. 1. Circuit configurations and schematic diagrams of E-field distribution for uniplanar tee junction. (a) In-phase CPW-slotline tee junction. (b) Out-of-phase CPW-slotline tee junction.

conductor. The CPW-to-slotline transition on the left CPW arm will produce an E-field in the positive y-direction at port 1. However, the transition on the right CPW arm will produce a negative y-directed slotline E-field at port 2. On the other hand, the in-phase tee junction as shown in Fig. 1(a) consists of two slotline arms separated by a CPW feed line. The E-field fed to CPW produces two in-phase slotline waves to output at ports 1 and 2.

Based on the above principle, an out-of-phase CPW-slotline tee junction was built on a 1.524 mm-thick RT/Duroid 6010 ($\varepsilon_r = 10.5$) substrate with characteristic impedances: $Z_{co} = 50\ \Omega$ for the CPW feed line, $Z_c = 66.9\ \Omega$ for the CPW arms, and $Z_s = 66.9\ \Omega$ for the slotline. Fig. 2 shows the measured amplitude and phase differences. The maximum amplitude difference is 0.35 dB from 1.8–7.9 GHz. The maximum phase deviation from 180° is 2.5° over the frequency range from 1–7.5 GHz.

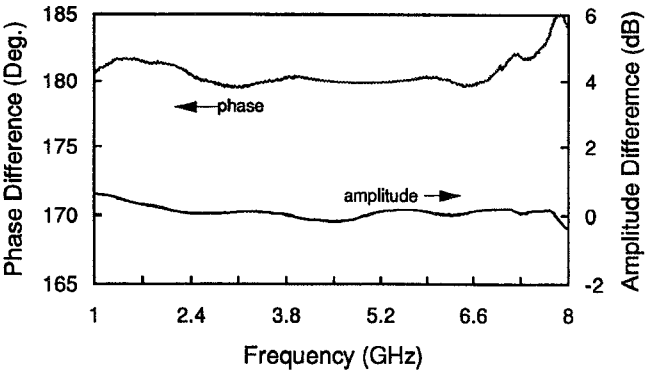

Fig. 2. Measured amplitude and phase differences for the out-of-phase CPW-slotline tee junction.

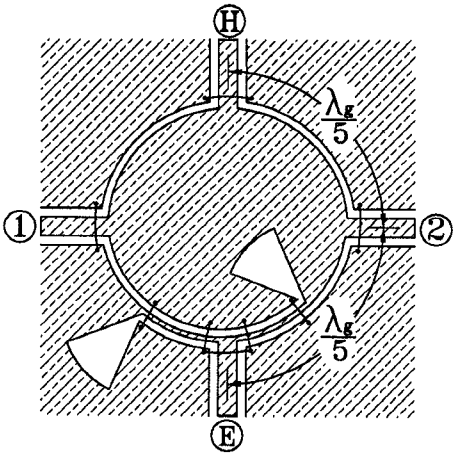

(a)

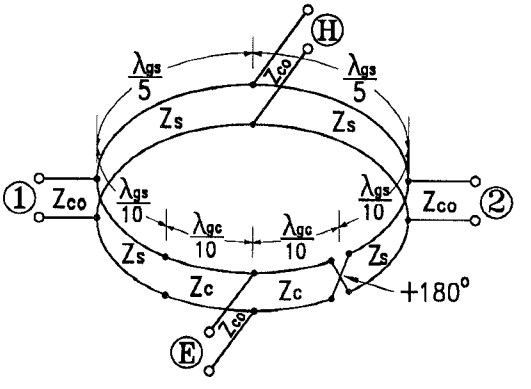

(b)

Fig. 3. Reduced-size uniplanar hybrid magic-T. (a) Circuit configuration and (b) equivalent transmission line model.

B. Reduced-Size Uniplanar Magic-T

Fig. 3(a) shows the circuit configuration of the new magic-T consisting of one out-of-phase and three in-phase CPW-slotline tee junctions. The out-of-phase T-junction serves as a phase inverter. In Fig. 3(a), ports E and H correspond to the E- and H-arm of the conventional waveguide magic-T, respectively. Ports 1 and 2 are the balanced arms. Fig. 3(b) shows the equivalent transmission line model of the magic-T. The twisted transmission line represents the phase reversal of the CPW-slotline T-junction.

Figs. 4 and 5 show the schematic diagram of the E-field distribution and the equivalent circuit for the in-phase and the out-of-phase coupling, respectively. In Fig. 4(a), the signal is fed to port H, which then divides into two components,

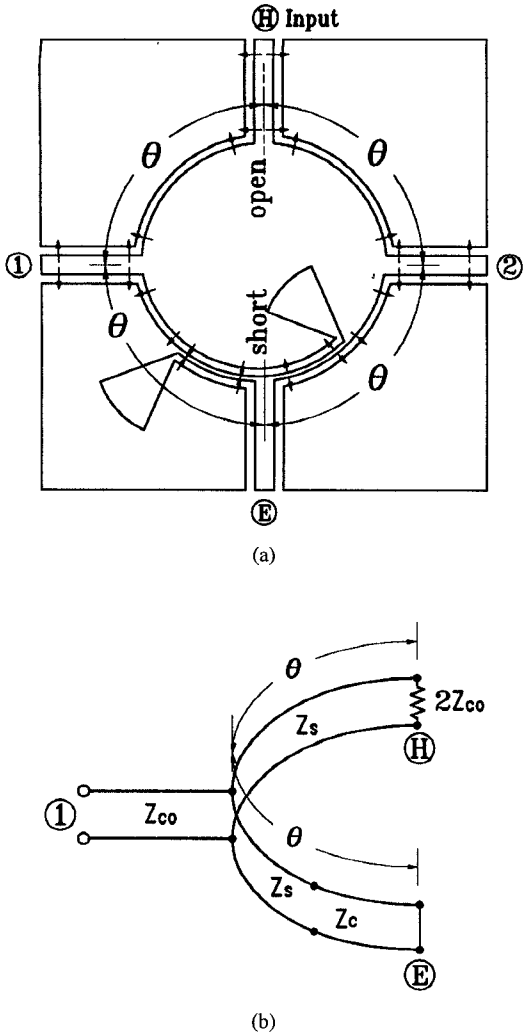

Fig. 4. (a) Schematic diagram of E-field distribution and (b) equivalent circuit for the out-of-phase coupling mode of the magic-T.

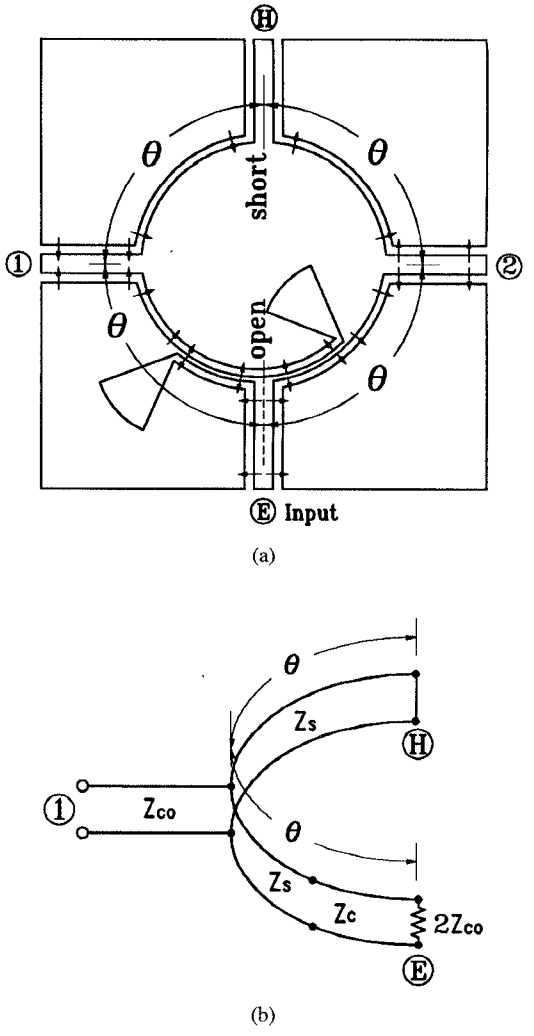

Fig. 5. (a) Schematic diagram of E-field distribution and (b) equivalent circuit for the in-phase coupling mode of the magic-T.

that both arrive in-phase at ports 1 and 2. However, the two components arrive at port E, out-of-phase and cancel out each other. In this case, the symmetry plane at port H corresponds to an open circuit (magnetic wall), while the symmetry plane at port E corresponds to a short circuit (electric wall). In Fig. 5(a), the signal is fed to port E, and then divides into two components, which arrive at ports 1 and 2 with a 180° phase difference. The 180° phase difference between the divided signals at ports 1 and 2 is due to the out-of-phase tee junction. The two component waves arrive at port H out-of-phase and cancel out each other. The symmetry plane at port E corresponds to an open circuit (magnetic wall); whereas the symmetry plane at port H corresponds to a short circuit (electric wall). The isolation between ports E and H is perfect as long as the phase reversal in the out-of phase CPW-slotline T-junction is ideal.

As shown in Figs. 4(b) and 5(b), an equivalent circuit was used to analyze the impedance matching. The characteristic impedance of slotline Z_s and CPW Z_c in terms of CPW feed line impedance Z_{co} (usually 50 Ω) and θ (the electric length of a quarter of the slotline ring circumference) are given by [15]

$$Z_s = Z_c = Z_{co}\sqrt{2(1-\cot^2\theta)}. \tag{1}$$

According to (1), the minimum θ is obviously 45°. Simulations indicate that wide band operation is obtained for values of θ which are smaller in the allowed range. In this design $\theta = 72°$ (i.e. $\lambda_g/5$) was chosen, resulting in the characteristic impedances $Z_s, Z_c = 66.9\ \Omega$. The magic-T has been fabricated on a RT/Duroid 6010 substrate ($\varepsilon_r = 10.5$, substrate thickness h =1.54 mm, metal thickness $t = 18\ \mu$m). The center frequency is 4.0 GHz. The radius of the radial stub at the CPW-slotline transitions is 5 mm. The radial stub angle is 45°. It is important to use air bridges at the magic-T's discontinuities to prevent the coupled slotline mode from propagating on the CPW lines. The measurements were made on an HP-8510 network analyzer using standard SMA connectors. The insertion loss includes two coaxial-to-CPW transitions. Touchstone software was used to simulate the circuit.

Fig. 6 shows the magic-T's measured and calculated transmission, return loss and isolation, respectively. For the E-

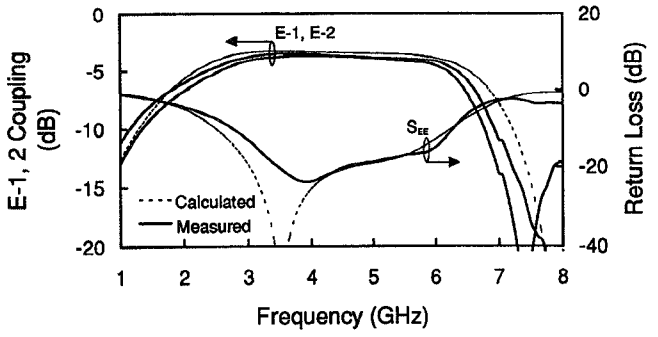

(a)

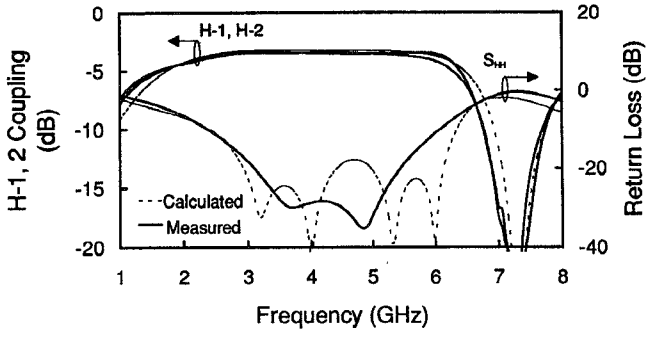

(b)

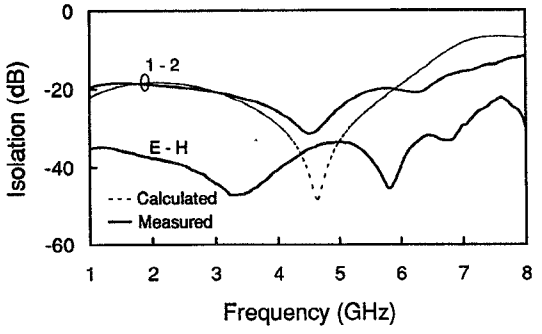

(c)

Fig. 6. Measured and calculated frequency responses of the magic-T. (a) Out-of-phase coupling of E-1, E-2, and E-port's return loss. (b) In-phase coupling of H-1, H-2, and H-port's return loss. (c) Isolations of E-H and 1-2.

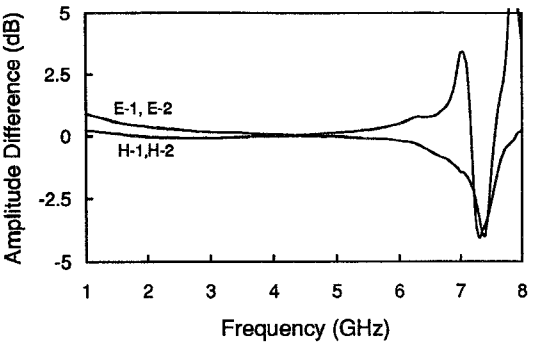

(a)

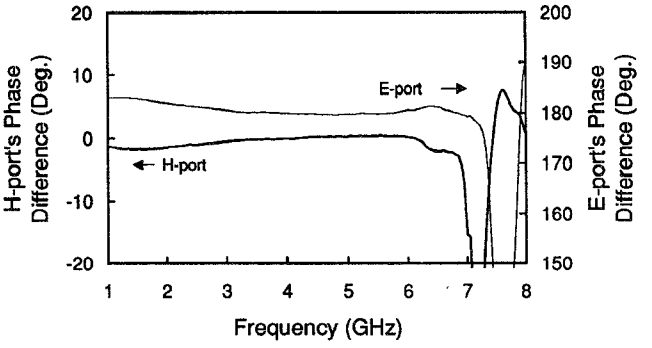

(b)

Fig. 7. Measured frequency responses of the magic-T. (a) Amplitude imbalance. (b) Phase imbalance.

TABLE I
SUMMARY OF MEASURED PERFORMANCES OF THE MAGIC-T

Parameter		Measured Result	Frequency Range (GHz)	Bandwidth (octave)
Coupling	fed to port E (S_{1E}, S_{2E})	3.9 ± 0.3 dB	2.8 - 5.9	> 1.075
	fed to port H (S_{1H}, S_{2H})	3.9 ± 0.3 dB	2.15 - 6.0	> 1.48
Return Loss	(S_{11}, S_{22}, S_{EE}, S_{HH})	> 15 dB	3.1 - 6.0	> 0.95
Isolation	port 1 and 2	> 18 dB	1.0 - 6.6	> 2.5
	port E and H	> 30 dB	1.0 - 7.7	> 2.5
Imbalance	amplitude E-1/E-2	< 0.4 dB	1.8 - 6.3	> 1.8
	amplitude H-1/H-2	< 0.4 dB	1.0 - 5.9	> 2.5
	phase E-1/E-2	181°±1.5°	2.0 - 7.15	> 1.8
	phase H-1/H-2	< 2.5°	1.0 - 6.4	> 2.5
Meeting All the above Specifications			3.1 - 5.9	> 0.93

port's power division (i.e., out-of-phase mode coupling) shown in Fig. 6(a), the insertion loss is less than 0.7 dB at the center frequency of 4 GHz. The return loss for the E-port is greater than 15 dB from 3.1–6.0 GHz. Similarly, Fig. 6(b) shows the insertion loss of 0.5 dB at the center frequency of 4 GHz for the H-port's power division (i.e., in-phase mode coupling). Also, the return loss for the H-port is greater than 15 dB from 2.7–6.2 GHz. The measured and calculated isolations between the E-port and H-port or ports 1 and 2 are shown in Fig. 6(c). As shown in Fig. 6, the calculated results agree very well with the measured results. Fig. 7 shows that the magic-T has a bandwidth of 1.6 octave from 2 to 6 GHz with a maximum power dividing imbalance of 0.4 dB and a 2.5° maximum phase imbalance. The measured performances of the various parameters are summarized in Table I.

III. REDUCED-SIZE 180° REVERSE-PHASE HYBRID-RING COUPLER

Hybrid couplers are indispensable components used in various MIC applications. The microstrip rat-race hybrid-ring coupler is a mature device and a commonly used 180° hybrid. Usually, the 20–26 percent bandwidth of this coupler limits its applications to narrow band circuits. Although several design techniques have been developed to extend the bandwidth [16]–[18], some disadvantages of using microstrip include the

precision fabrication for constructing the shorted coupled-line section [16], [17] and the difficulty of inserting the ground pins for the microstrip shorts [18]. Recently, uniplanar transmission lines have emerged as alternatives to microstrip in planar microwave integrated circuits. A narrow band uniplanar hybrid coupler [11] was proposed by Hirota *et al.* in 1987. The circuit is based on a slotline ring with three in-phase CPW feeds via an air bridge. More recently, two broad-band uniplanar hybrid-ring couplers [19], [20] operating over an octave bandwidth were developed using a one-wavelength cross-over slotline ring and a one-wavelength cross-over CPW ring structure. However, these devices consist of $\lambda/4$ sections that occupy large areas in MIC applications and the bandwidth is limited by the electrical line length. To overcome these problems for monolithic integration, a uniplanar reverse-phase hybrid-ring coupler is described here using a CPW-slotline ring with a 180° reverse-phase CPW-slotline back-to-back balun and four CPW feeds. Since the 180° phase change of the CPW-slotline balun is frequency independent, the reverse-phase hybrid-ring coupler has the advantages of uniplanar structure, small size, and broadband operation.

Fig. 8(a) shows the circuit layout of the reduced-size uniplanar hybrid-ring coupler. The circuits consist of four CPW-slotline tee junctions and one 180° reverse-phase CPW- slotline back-to-back balun which is formed using a pair of CPW-to-slotline transitions as shown in Fig. 8(a). Fig. 8(b) shows the equivalent transmission line model. The twisted transmission line represents the 180° reverse-phase CPW-slotline back-to-back balun.

Similarly to the case of magic-T in Section II, the characteristic impedance of slotline Z_s and CPW Z_c in terms of CPW feed line impedance Z_{co} and θ are given by (1). In this design, $\theta = 72°$ (i.e., $\lambda_{gs}/5$) was chosen resulting in the characteristic impedances Z_s and $Z_c = 66.9\ \Omega$. The hybrid-ring coupler was fabricated on a 1.524 mm-thick RT/Duroid 6010 ($\varepsilon_r = 10.5$) substrate. The dimensions are listed as follows

coupler's circumference: $C = 0.8\lambda_g$
(mean radius $R = 4.52$ mm)
slotline ring: $Z_s = 66.9\ \Omega$ (slotline width $W_s = 0.31$ mm)
CPW section: $Z_c = 66.9\ \Omega$ (center strip $S_c = 0.2$ mm,
gap size $G_c = 0.31$ mm)
CPW feed ines: $Z_{co} = 50\ \Omega$ (center strip $S_{co} = 0.6$ mm,
gap size $G_{co} = 0.31$ mm)
slotline radial stub radius: $r_s = 5$ mm
slotline radial stub angle: $\varphi_s = 45°$.

To eliminate the coupled slotline mode propagating on the CPW lines, bonding wires have been used at the coupler's CPW-slotline discontinuities. The measurements were made on an HP-8510 network analyzer using standard SMA connectors. The insertion loss includes two coaxial-to-CPW transitions.

Fig. 9 shows the hybrid-ring coupler's measured frequency responses of coupling, isolation, return loss, amplitude and phase imbalance, respectively. The measured results show that the couplings of the power from port 1 to ports 2 and 3 are 3.6 and 3.7 dB at 4 GHz, respectively. The isolation between ports 1 and 4 is greater than 19 dB, and return loss is more than 15 dB both over a frequency range from 2.7–6 GHz. The amplitude and phase imbalance between ports 2 and 3 are excellent over a broad bandwidth. The reduction of the line length to 72° has no deleterious effect on performance of the circuit. However, the radial stub in the center of the ring can cause problem for the smaller circumference. The coupler's measured performances are listed in Table II.

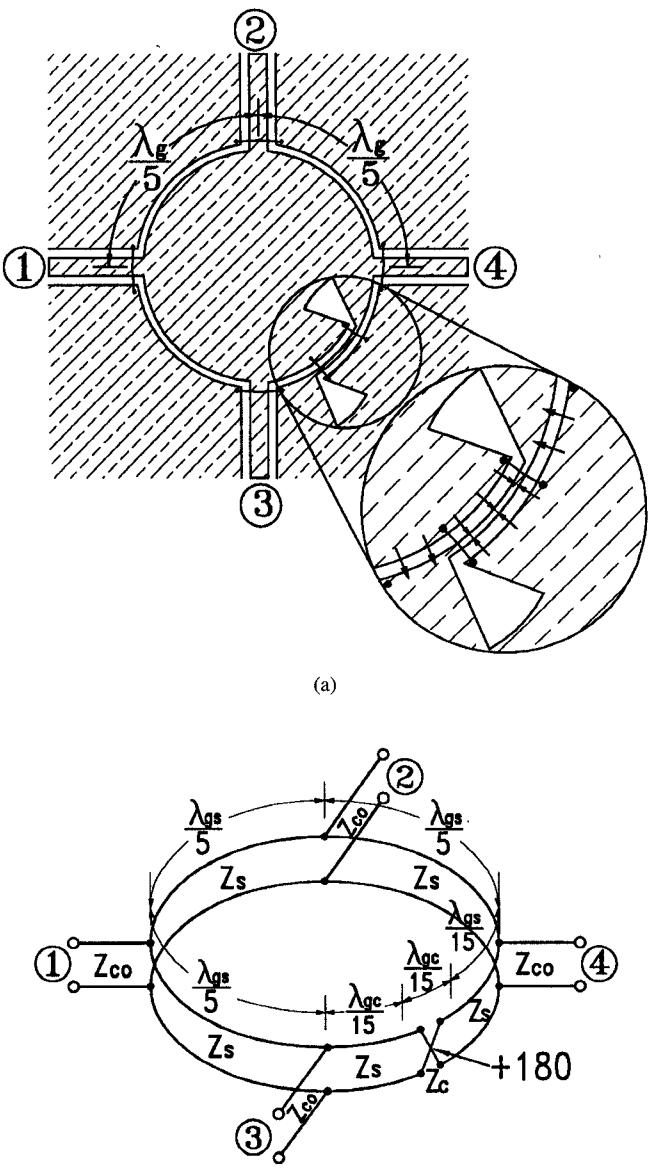

Fig. 8. Reduced-size reverse-phase hybrid-ring coupler. (a) Circuit configuration. (b) Equivalent transmission line model.

IV. Uniplanar de Ronde's CPW-Slot Coupler

Parallel-coupled transmission-line directional couplers, Lange couplers, and branch-line couplers are the fundamental 90° hybrids used in many printed microwave integrated circuits. In 1970 de Ronde [21] proposed a new coupler structure with a strip on top of the substrate and a slot in the ground plane. The de Ronde's strip-slot directional coupler

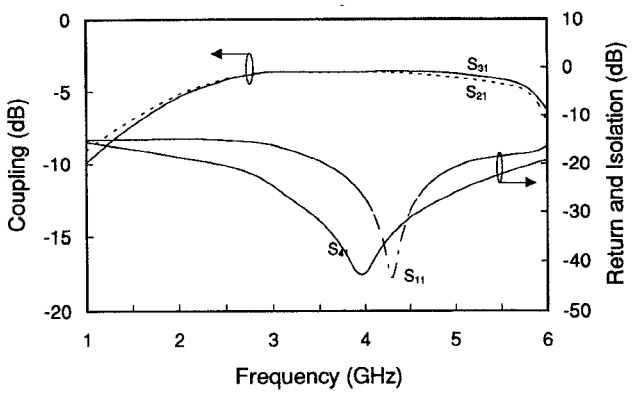

Fig. 9. Measured frequency responses of the hybrid-ring coupler. (a) Coupling, return loss, and isolation. (b) Amplitude imbalance and phase imbalance.

TABLE II
SUMMARY OF MEASURED PERFORMANCES OF THE HYBRID-RING COUPLER

Parameter		Measured Result	Frequency Range (GHz)	Bandwidth (octave)
Coupling	(S_{21}, S_{31})	3.9 ± 0.3 dB	2.5 - 5.3	> 1.1
Isolation	(S_{41})	> 19 dB	2.0 - 6.0	> 1.6
Return Loss	(S_{11}, S_{22}, S_{33}, S_{44})	> 15 dB	2.7 - 6.0	> 1.2
Imbalance	amplitude($\|S_{21}\|/\|S_{31}\|$)	< 0.4 dB	1.6 - 5.8	> 1.85
	phase ($\angle S_{21} - \angle S_{31}$)	< 2.5°	2.4 - 6.0	> 1.3
Meeting All the above Specifications			2.7 - 5.3	> 0.97

can easily achieve 3 dB coupling. An empirical optimization technique for the de Ronde's strip-slot directional coupler was published by Garcia [22]. In 1974, Shiek [23] first analyzed the de Ronde's strip-slot directional coupler with the aid of an equivalent circuit of the branch-line coupler. The analysis showed that the de Ronde's strip-slot directional coupler is just a special case of the 3-branch directional coupler. In 1982, Hoffmann and Siegl [24] proposed a complete analysis of de Ronde's directional coupler using even-odd mode analysis of four-port networks with double symmetry. The scattering parameters of the couplers were

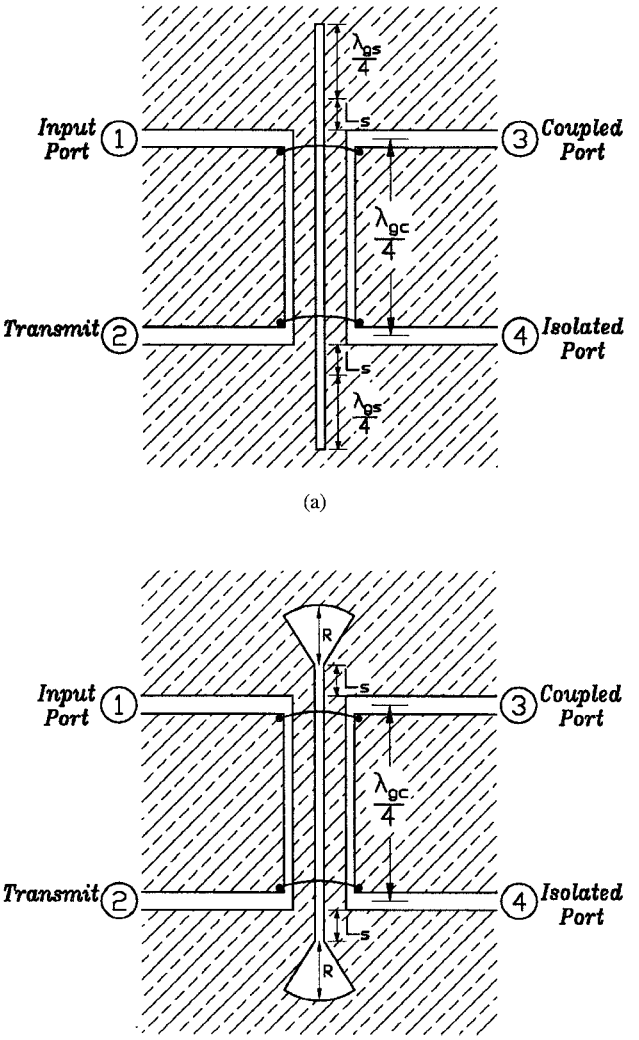

Fig. 10. Configuration of the uniplanar de Ronde's CPW-slot directional coupler with (a) $\lambda_{gs}/4$ slotline short stubs and (b) slotline radial stubs on both ends of the slot-mode-excited coupling section.

derived and the compensated couplers were also demonstrated. Recently, Schoenberger *et al.* [25] presented a slot-strip finline coupler which is complementary to the de Ronde's strip-slot directional coupler.

This section describes a new uniplanar de Ronde's CPW-slot directional coupler. The new coupler uses parallel and series CPW-slotline connections. Both the CPW and slotline are on the same side of substrate. A truly uniplanar de Ronde's CPW-slot directional coupler with 5 dB coupling was demonstrated for use from 2.4–3.4 GHz. The experimental results agree with the theoretical design.

Fig. 10 shows the physical configurations of the uniplanar de Ronde's CPW slot directional couplers. The new couplers consist of a section of a CPW and a slotline which are in close proximity and are continuously coupled. The slotline coupling section with a compensation length L_S is terminated with a $\lambda_{gs}/4$ slotline short stub or a slotline radial stub on both ends, as shown in Fig. 10(a) and (b), respectively. The purpose of adding an extended slotline section L_S is to compensate

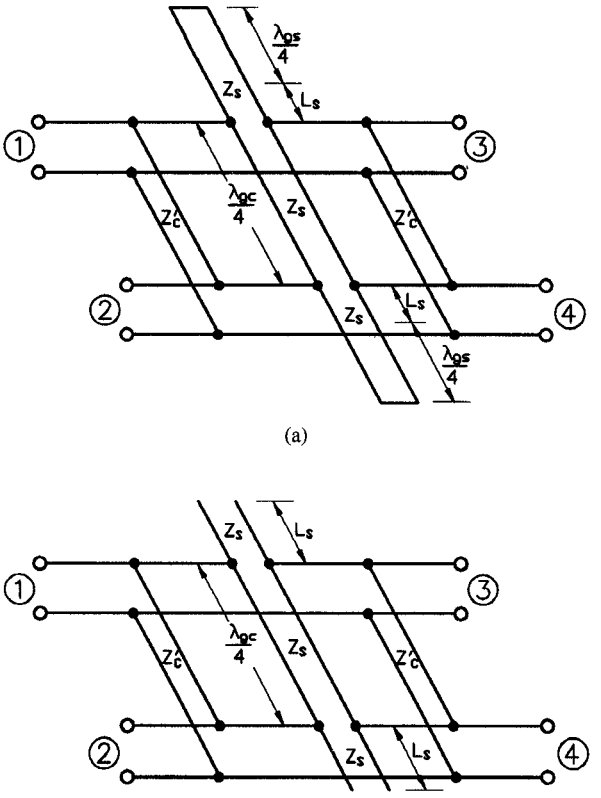

Fig. 11. Equivalent transmission line model for the coupler in Fig. 10 with (a) $\lambda_{gs}/4$ slotline short stubs and (b) slotline radial stubs on both ends of the slot-mode-excited coupling section.

for the difference of phase velocity between the even- and odd-mode coupling. The output four ports are formed by two CPW-slotline tee junctions. Fig. 11 shows the equivalent transmission line models. The CPW-mode-excited coupling section in Fig. 11 is modeled by a parallel connection of two transmission lines with characteristic impedance $Z_C' = 2Z_C$, where Z_C is the characteristic impedance of the coplanar waveguide in Fig. 10. The slot-mode-excited coupling section is modeled by a series connection of a transmission line with a characteristic impedance of Z_S.

To analyze the uniplanar de Ronde's coupler, the even-odd mode analysis of four-port networks with double symmetry proposed by Hoffmann and Siegl [24] is used. Fig. 12 shows the common four-port network with respect to planes P_1 P_1 and P_2 P_2. The scattering parameters S_{ij} can be expressed by even-odd mode excitations as [24]

$$S_{11} = \frac{\Gamma_{ee} + \Gamma_{eo} + \Gamma_{oe} + \Gamma_{oo}}{4} \tag{2a}$$

$$S_{21} = \frac{\Gamma_{ee} - \Gamma_{eo} + \Gamma_{oe} - \Gamma_{oo}}{4} \tag{2b}$$

$$S_{31} = \frac{\Gamma_{ee} + \Gamma_{eo} - \Gamma_{oe} - \Gamma_{oo}}{4} \tag{2c}$$

$$S_{41} = \frac{\Gamma_{ee} - \Gamma_{eo} + \Gamma_{oe} - \Gamma_{oo}}{4} \tag{2d}$$

where $\Gamma_{ee}, \Gamma_{eo}, \Gamma_{oe}$, and Γ_{oo} represent the input reflection coefficients with certain combinations of even- and odd-mode

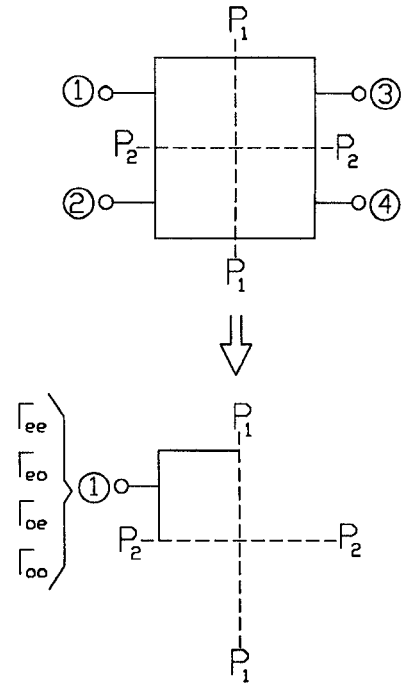

Fig. 12. Configuration of the common four-port network with double symmetry with respect to planes P_1 P_1 and P_2 P_2.

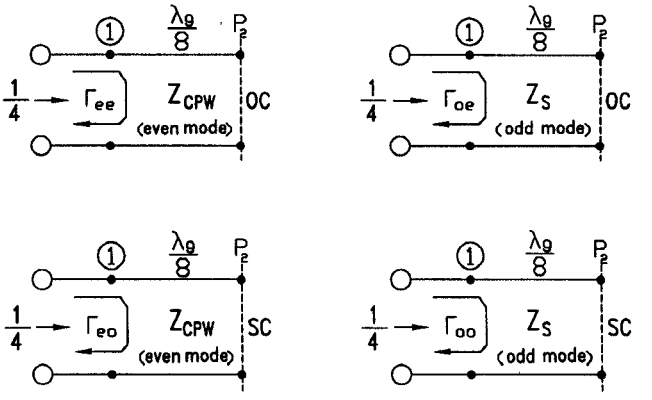

Fig. 13. Schematic expression of the reflection coefficients with double symmetry in the uniplanar de Ronde's coupler.

excitations at ports 1–4. The first subscript $e(o)$ denotes the combination of even- and odd-mode excitations at ports 1–4 making an open(short) circuit at the symmetry plane P_1 P_1. The second subscript $e(o)$ denotes the combination of even- and odd-mode excitations at ports 1–4 making an open(short) circuit at the symmetry plane P_2 P_2. Fig. 13 shows the definition of the reflection coefficients with double symmetry in the uniplanar de Ronde's coupler.

Characteristic impedances of the coupler lines in terms of coupling coefficient are given by [24]

$$Z_c = \frac{Z_0}{2}\sqrt{\frac{1+C}{1-C}} \tag{3}$$

$$Z_s = 2Z_0\sqrt{\frac{1-C}{1+C}} \tag{4}$$

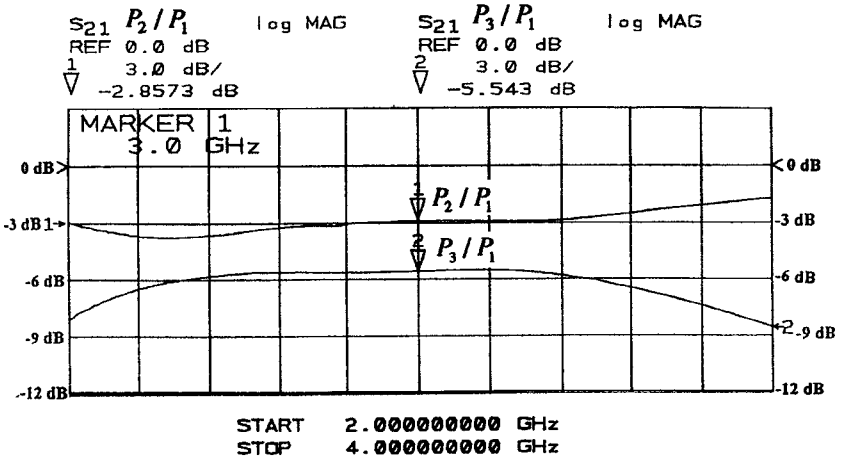

(a)

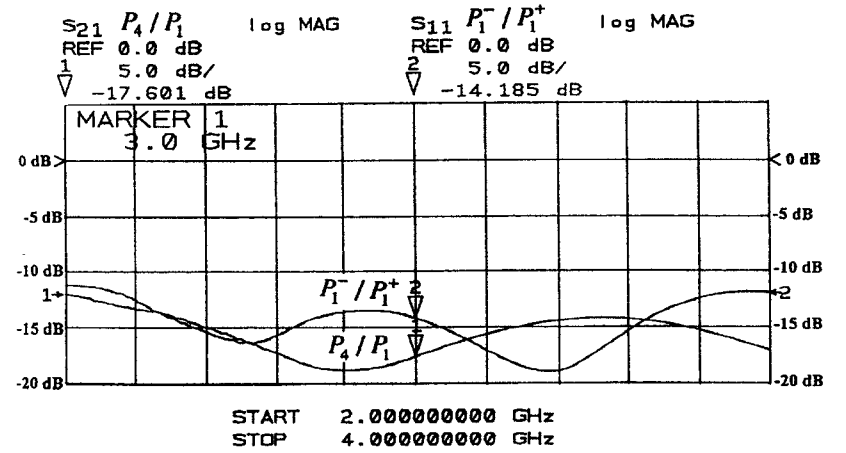

(b)

Fig. 14. Measured frequency responses of (a) power transmitting and coupling, and (b) return loss and isolation for the uniplanar de Ronde's CPW-slot directional coupler with 5 dB coupling.

where Z_0 is the terminating impedance, Z_C is the characteristic impedance of coplanar waveguide, Z_S is the characteristic impedance of slotline, and C is the coupling coefficient. According to synthesis (3) and (4), a truly uniplanar de Ronde's CPW-slot directional coupler, as shown in Fig. 10(b), with 5 dB coupling was built on a RT/Duroid 6010.8 ($\varepsilon_r = 10.8$) substrate with the following dimensions: substrate thickness h =1.524 mm, impedance of the slotline feeds $Z_{S0} = 50.82\ \Omega$, slotline feeds line width $W_{S0} = 0.07$ mm, CPW impedance $Z_C = 47.21\ \Omega$, CPW center conductor width $S_C = 0.43$ mm, CPW gap size $G_C = 0.23$ mm, length of the CPW-slot coupling section $\lambda_{gc}/4 = 10.57$ mm, impedance of the slotline coupling section $Z_S = 53.0\ \Omega$, line width of the slotline coupling section $W_S = 0.094$ mm, radius of the slotline radial stub $r = 6$ mm, and angle of the slotline radial stub $\theta = 60°$.

To test the coupler, a wide-band CPW-slotline transition [26] was used to connect to ports 1–4. The measurements were made using standard SMA connectors and an HP-8510 network analyzer. Fig. 14(a) shows the measured frequency responses of power transmitting and coupling. The power coupling is 5.55 dB (including insertion loss) at the center frequency of 3 GHz. Fig. 14(b) shows the measured return loss and isolation between ports 1 and 4. The return loss is more than 14 dB and the isolation is more than 17 dB at the center frequency. The poor return loss is duo to the mechanical tolerances, misalignments and connectors. Fig. 15 shows phase angles of ports 2 and 3. The phase difference between ports 2 and 3 is 90.3° at the center frequency, and 90° ± 7° in the frequency range from 2–4 GHz. The 5 dB uniplanar de Ronde's CPW-slot directional coupler provides good coupling and phase performance as predicted.

V. Conclusion

New reduced-size, wide-band uniplanar magic-T and reverse-phase hybrid-ring were developed. Both use the combination of CPWs and slotlines on one side of the substrate with CPW feeds. They have a CPW-slotline ring circumference of only $0.8\lambda_g$ which is 20% smaller compared to the size of conventional couplers. The magic-T and

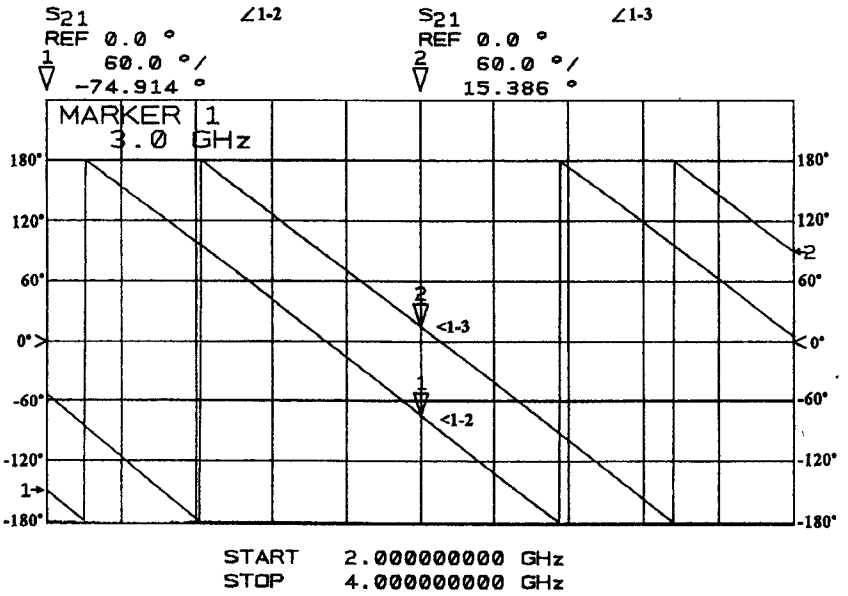

Fig. 15. Measured frequency responses of phase angles for the uniplanar de Ronde's CPW-slot directional coupler with 5 dB coupling.

hybrid-ring coupler demonstrated good performances and excellent output amplitude and phase balance over bandwidth of 1.6 and 1.3 octave, respectively. Experimental results agree well with the simulated ones. In addition, a new 5 dB uniplanar de Ronde's CPW-slot directional coupler was demonstrated and the experimental results showed good coupling and phase performances as predicted. With the advantages of wide band operation, small size, uniplanar structure and easy integration with solid-state devices, these circuits should be useful components for many applications in microwave hybrid and monolithic integrated circuits. However, the return loss bandwidth of these circuits needs to be improved.

REFERENCES

[1] M. A. Tuko and I. Wolff, "Novel 36 GHz GaAs frequency doublers using (M)MIC coplanar technology," in *IEEE MTT-S Int. Microwave Symp. Dig.*, 1992, pp. 1167–1170.

[2] D. Cahana, "A new coplanar waveguide/slotline double-balanced mixer," in *IEEE MTT-S Int. Microwave Symp. Dig.*, 1989, pp. 967–968.

[3] T. Hirota and H. Ogawa, "Uniplanar monolithic frequency doublers," *IEEE Trans. Microwave Theory Tech.*, vol. 37, pp. 1249–1254, Aug. 1989.

[4] C. H. Ho, L. Fan, and K. Chang, "Broad-band uniplanar hybrid-ring coupler," *Elect. Lett.*, vol. 29, pp. 44–45, Jan. 1993.

[5] Y. H. Shu, J. A. Navarro, and K. Chang, "Electronically switchable and tunable coplanar waveguide-slotline band-pass filter," *IEEE Trans. Microwave Theory Tech.*, vol. 39, pp. 548–554, Mar. 1991.

[6] T. Hirota, Y. Tarusawa, H. Ogawa, and K. Owada, "Planar MMIC hybrid circuit and frequency converter," in *IEEE MTT-S Int. Microwave Symp. Dig.*, 1986, pp. 103–105.

[7] M. Aikawa and H. Ogawa, "Double-sized MIC's and their applications," *IEEE Trans. Microwave Theory Tech.*, vol. 37, pp. 406–413, Feb. 1989.

[8] T. Tokumitsu, S. Hara, and M. Aikawa, "Very small ultra-wide-band MMIC magic-T and applications to combiners and dividers," *IEEE Trans. Microwave Theory Tech.*, vol. 37, pp. 1985–1990, Dec. 1989.

[9] D. I. Kim and Y. Naito, "Broad-band design of improved hybrid-ring 3-dB directional coupler," *IEEE Trans. Microwave Theory Tech.*, vol. MTT-30, pp. 2040–2046, Nov. 1982.

[10] D. I. Kim and G. S. Yang, "Design of a new hybrid-ring directional coupler using $\lambda/8$ or $\lambda/6$ section," *IEEE Trans. Microwave Theory Tech.*, vol. 39, pp. 1779–1783, Oct. 1991.

[11] T. Hirota, Y. Tarusawa, and H. Ogawa, "Uniplanar MMIC hybrids—A proposed new MMIC structure," *IEEE Trans. Microwave Theory Tech.*, vol. MTT-35, pp. 576–581, June 1987.

[12] C. H. Ho, L. Fan, and K. Chang, "A broad-band uniplanar slotline hybrid ring coupler with over one octave bandwidth," in *IEEE MTT-S Int. Microwave Symp. Dig.*, 1993, pp. 585–588.

[13] ——, "New uniplanar coplanar waveguide couplers," in *IEEE MTT-S Int. Microwave Symp. Dig.*, 1994, pp. 285–288.

[14] K. Hettak, J. P. Coupez, A. Sheta, T. Le Gouguec, and S. Toutain, "Practical design of uniplanar broadband subsystems application to a wideband hybrid magic tee," in *IEEE MTT-S Int. Microwave Symp. Dig.*, 1994, pp. 915–918.

[15] M.-H. Murgulescu, E. Moisan, P. Legaud, E. Penard, and I. Zaquine, "New wideband, $0.67\lambda_g$ circumference 180° hybrid ring coupler," *Elect. Lett.*, vol. 30, pp. 299–300, Feb. 1994.

[16] S. J. Robinson, "Broad-band hybrid junctions," *IRE Trans. Microwave Theory Tech.*, vol. MTT-8, pp. 671–672, Nov. 1960.

[17] S. March, "A wide band stripline hybrid ring," *IEEE Trans. Microwave Theory Tech.*, vol. MTT-16, p. 361, June 1968.

[18] L. W. Chua, "New broad-band matched hybrids for microwave integrated circuits," in *1971 Proc. of The European Microwave Conf.*, 1971, pp. C4/5:1–C4/5:4.

[19] C. H. Ho, L. Fan, and K. Chang, "Broad-band uniplanar hybrid-ring and branch-line couplers," *IEEE Trans. Microwave Theory Tech.*, vol. 41, pp. 2116–2125, Dec. 1993.

[20] ——, "New uniplanar coplanar waveguide hybrid-ring couplers and magic-Ts," *IEEE Trans. Microwave Theory Tech.*, vol. 42, pp. 2440–2448, Dec. 1994.

[21] F. C. de Ronde, "A new class of microstrip directional couplers," in *IEEE MTT-S Int. Microwave Symp. Dig.*, 1970, pp. 184–186.

[22] J. A. Garcia, "A wide-band quadrature hybrid coupler," *IEEE Trans. Microwave Theory Tech.*, vol. MTT-19, pp. 660–661, July 1971.

[23] B. Shiek, "Hybrid branch-line couplers-a useful new class of directional couplers," *IEEE Trans. Microwave Theory Tech.*, vol. MTT-22, pp. 864–869, Oct. 1974.

[24] R. K. Hoffmann and J. Siegl, "Microstrip-slot coupler design," Parts I and II. *IEEE Trans. Microwave Theory Tech.*, vol. MTT-30, pp. 1205–1216, Aug. 1982.

[25] M. Schoenberger, A. Biswas, A. Mortazawi, and V. K. Tripathi, "Coupled slot-strip coupler in finline," in *IEEE MTT-S Int. Microwave Symp. Dig.*, 1991, pp. 751–753.

[26] C. H. Ho, L. Fan, and K. Chang, "Experimental investigation of CPW-slotline transitions for uniplanar microwave integrated circuits," in *IEEE MTT-S Int. Microwave Symp. Dig.*, 1993, pp. 877–880.

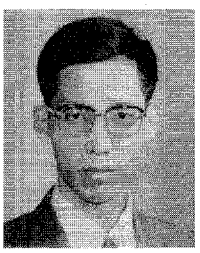

Lu Fan received the B.S. degree in electrical engineering from Nanjing Institute of Technology (currently Southeast University), Nanjing, China, in 1982.

From September 1982 to December 1990, he was with the Department of Radio Engineering of Nanjing Institute of Technology as a teaching assistant and lecturer. In January 1991, he became a Research Associate in the Department of Electrical Engineering, Texas A&M University, College Station, TX. His research interests include microwave and millimeter-wave components and active antennas.

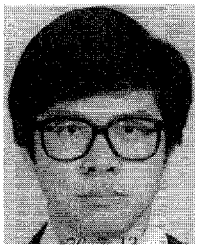

Chien-Hsun Ho was born in Kaohsung, Taiwan, on October 9, 1963. He received the B.S.E.E. and M.S. degrees from the National Taiwan University, Taipei, Taiwan, and the Ph.D. degree from the Texas A&M University, College Station, TX, in 1985, 1987, and 1993, respectively.

From 1990 to 1993 he worked for the Microwave Laboratory, Texas A&M University, as a Research Assistant. He joined the Garmin Communication and Navigation Co. in January 1994 as a Development Engineer. His research interests include microwave integrated circuits and antennas.

Sridhar Kanamaluru (S'93) received the B.E. degree from Anna University, Madras, India in 1987 and the M.S. degree from Texas A&M University in 1993. He is currently pursuing his Ph.D. degree at Texas A&M University. His present research includes analysis of aperture coupled microstrip antennas fed by dielectric image lines and CPW/slotline uniplanar circuits.

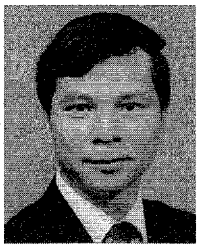

Kai Chang (S'75–M'76–SM'85–F'91) received his B.S.E.E. degree from the National Taiwan University, Taipei, Taiwan, the M.S. degree from the State University of New York at Stony Brook, and the Ph.D. degree from the University of Michigan, Ann Arbor, in 1970, 1972, and 1976, respectively.

From 1972 to 1976, he worked for the Microwave Solid-State Circuits Group, Cooley Electronics Laboratory of the University of Michigan as a Research Assistant. From 1976 to 1978, he was employed by Shared Applications, Inc., Ann Arbor, where he worked in computer simulation of microwave circuits and microwave tubes. From 1978 to 1981, he worked for the Electron Dynamics Division, Hughes Aircraft Company, Torrance, CA, where he was involved in the research and development of millimeter-wave solid-state devices and circuits, power combiners, oscillators and transmitters. From 1981 to 1985, he worked for the TRW Electronics and Defense, Redondo Beach, CA, as a Section Head, developing state-of-the-art millimeter-wave integrated circuits and subsystems including mixers, VCOs, transmitters, amplifiers, modulators, upconverters, switches, multipliers, receivers, and transceivers. He joined the Electrical Engineering Department of Texas A&M University in August 1985 as an Associate Professor and was promoted to a Professor in 1988. In January 1990, he was appointed E-Systems Endowed Professor of Electrical Engineering. His current interests are in microwave and millimeter-wave devices and circuits, microwave integrated circuits, microwave optical interactions, and antennas. He authored a book, "Microwave Solid-State Circuits and Applications" (New York: Wiley, 1994). He served as the editor of the four-volume "Handbook of Microwave and Optical Components" published by Wiley in 1989 and 1990. He is the editor of the MICROWAVE AND OPTICAL TECHNOLOGY LETTERS and the WILEY BOOK SERIES IN MICROWAVE AND OPTICAL ENGINEERING. He has published over 200 technical papers and several book chapters in the areas of microwave and millimeter-wave devices and circuits.

Dr. Chang received the Special Achievement Award from TRW in 1984, the Halliburton Professor Award in 1988, the Distinguished Teaching Award in 1989, and the Distinguished Research Award in 1992 from the Texas A&M University.